

Ab initio investigation of Ti₂Al(C,N) solid solutions

Raymundo Arróyave* and Miladin Radovic

Department of Mechanical Engineering, Texas A&M University, College Station, Texas 77843-3123 and United States and Materials Science and Engineering Program, Texas A&M University, College Station, Texas 77843-3123, United States

(Received 19 September 2011; published 24 October 2011)

$M_{n+1}AX_n$ phases (M: early transition metal, A: IIIA- or IVA-group element, X: carbon or nitrogen) are layered ternary compounds that possess both metal- and ceramic-like properties with numerous potential applications in bulk and thin film forms, particularly under high-temperature conditions. In this work, we use the cluster expansion formalism to investigate the energetics of C-N interactions across the entire Ti₂AlC-Ti₂AlN composition range. It is shown that there is a definite tendency for ordering in the C,N sublattice. However, the molar volume and bulk modulus of the ordered structures found along the Ti₂AlC-Ti₂AlN composition range show small deviations from the (linear) rule of mixing, indicating that despite the ordering tendencies, the C-N interactions are not strong and the solution becomes disordered at relatively low temperatures. Random solid solutions of Ti₂AlC_{1-x}N_x are simulated using special quasirandom structures (SQS) with $x = 0.25, 0.50,$ and 0.75 . The thermodynamic properties of these structures are compared to those of the structures found to belong to the ground state through the cluster expansion approach. It is found that the structural properties of these approximations to random alloys do not deviate significantly from Vegard's law. The trend in the structural parameters of these SQS are found to agree well with available experimental data and the predictions of the bulk modulus suggest a very weak alloying effect—with respect to Vegard's law—on the elastic properties of Ti₂AlC_{1-x}N_x.

DOI: [10.1103/PhysRevB.84.134112](https://doi.org/10.1103/PhysRevB.84.134112)

PACS number(s): 81.05.Je, 71.15.Mb, 81.30.Bx, 82.60.Lf

I. INTRODUCTION

$M_{n+1}AX_n$ phases (M: early transition metal, A: IIIA- or IVA-group element, X: carbon or nitrogen) are interesting types of layered ternary compounds that possess both metal- and ceramic-like properties. While they show the machinability, thermal-shock resistance, damage tolerance, and electrical and thermal conductivity of metals, they are similar to ceramics in terms of their high stiffness, corrosion, and oxidation resistance.¹⁻⁴

Among the more than 70 $M_{n+1}AX_n$ phases synthesized to date, Ti₂AlC and Ti₂AlN and their solid solutions are perhaps the best characterized ones. The synthesis of bulk polycrystalline samples of these two ternary alloys was reported by Barsoum and his group in 1997.⁵ Since then, several experimental and theoretical studies have addressed different structural aspects and mechanical properties of Ti₂AlC, Ti₂AlN, and their solid solutions.⁶⁻¹⁴ Recently, there have been a number of theoretical works investigating the thermodynamic properties of the Ti₂Al(C,N) system. For example, Drulis *et al.* studied the heat capacity of Ti₂AlC_{0.5}N_{0.5}.¹⁵ In a similar work, Scabarozzi *et al.* compared the specific heats of Ti₃Al(C_{0.5}N_{0.5})₂, Ti₂AlC_{0.5}N_{0.5}, and Ti₂AlN.¹⁶ More recently, Du and collaborators investigated the elastic properties of Ti₂AlC_{0.5}N_{0.5} solutions using theoretical means.¹⁷ As of now, and to the best of the knowledge of the authors, there are not many theoretical works addressing the nonstoichiometry of MAX phases in a systematic manner. Du's work,¹⁷ for example, approximated the Ti₂AlC_{0.5}N_{0.5} solution by simply setting a mixed occupancy (C and N) in the X sublattice of a Ti₂AlX structure. This model implicitly assumes that C-N interactions are not significant enough. The underlying assumption for this approximation cannot be assessed unless a systematic investigation of the alloying behavior of C and N in the X sublattice is carried out.

In this work, we address this issue by first investigating the energetics of the C-N alloying in the X sublattice using

the cluster-expansion formalism. The ground state of the Ti₂AlC-Ti₂AlN system is obtained and the alloying effects on some structural properties of these alloys are predicted using the properties calculated for structures derived from the underlying Ti₂Al(C,N) lattice. Furthermore, random solid solutions of Ti₂Al(C,N) are simulated using so-called special quasirandom structures (SQS)¹⁸ to mimic random arrangement among C-N within a limited coordination range. The electronic, structural, and mechanical properties of a select set of Ti₂Al(C,N) alloys with 25, 50, and 75 % compositions are investigated. The properties and energetics of the structures investigated are calculated using *ab initio* methods based on density functional theory.¹⁹ The available experimental data are used to evaluate the validity of the approach used and to gain a better insight on the underlying physical behavior responsible for the macroscopic properties of these alloys.

II. METHODOLOGY**A. Electronic structure calculations**

The total energy calculations were performed within the framework of the density functional theory,¹⁹ as implemented in the Vienna *ab initio* simulation package (VASP).^{20,21} The generalized gradient approximation (GGA) is used in the form of the parametrization proposed by Perdew, Burke, and Ernzerhof (PBE).^{22,23} The electronic configurations of titanium, aluminum, carbon, and nitrogen were chosen to be [Ar]3d³4s¹, [Ne]3s²3p¹, [Ar]3d¹⁰4s²4p¹, 1s²2s²2p², and 1s²2s²2p³, within the projector augmented-wave (PAW) pseudopotentials formalism,²⁴ implemented in the VASP package.^{25,26} The Brillouin zone integrations were performed using a Monkhorst-Pack mesh²⁷ with 5000 k points per reciprocal atom. Full relaxations were realized by using the Methfessel-Paxton smearing method of order one²⁸ and a final self-consistent static calculation with the tetrahedron smearing method with Blöchl corrections.²⁹ A cutoff energy of 520 eV was set for all

of the calculations and the spin polarizations were taken into account.

B. Elastic properties

The elastic constants were estimated by stress-strain approach^{30–36} where a set of strains $\varepsilon = (\varepsilon_1, \varepsilon_2, \varepsilon_3, \varepsilon_4, \varepsilon_5, \varepsilon_6)$ is imposed on a crystal structure. If \mathbf{A} is the lattice vectors specified in Cartesian coordinates, $\varepsilon_1, \varepsilon_2, \varepsilon_3$ and $\varepsilon_4, \varepsilon_5, \varepsilon_6$ are the normal strains and the shear strains, respectively. Then, the deformed lattice vectors are

$$\bar{\mathbf{A}} = \mathbf{A} \begin{pmatrix} 1 + \varepsilon_1 & \frac{\varepsilon_6}{2} & \frac{\varepsilon_5}{2} \\ \frac{\varepsilon_6}{2} & 1 + \varepsilon_2 & \frac{\varepsilon_4}{2} \\ \frac{\varepsilon_5}{2} & \frac{\varepsilon_4}{2} & 1 + \varepsilon_3 \end{pmatrix}. \quad (1)$$

After the application of the strain, it is possible to obtain the set of stresses \mathbf{t} , which result from the changes on the energy due to the deformation, which is calculated using DFT methods.

Applying Hooke's law ($t = \varepsilon C$), if a n set of strains ($\varepsilon_{1 \rightarrow n}$) are applied, the result is a set of stresses ($t_{1 \rightarrow n}$) which can be used to find the 6×6 elastic constant matrix (C) according to

$$\begin{pmatrix} C_{11} & \dots & C_{16} \\ \vdots & \ddots & \vdots \\ C_{61} & \dots & C_{66} \end{pmatrix} = \begin{pmatrix} \varepsilon_{1,1} & \dots & \varepsilon_{1,n} \\ \vdots & \ddots & \vdots \\ \varepsilon_{6,n} & \dots & \varepsilon_{6,n} \end{pmatrix}^{-1} \begin{pmatrix} t_{1,1} & \dots & t_{1,n} \\ \vdots & \ddots & \vdots \\ t_{6,1} & \dots & t_{6,n} \end{pmatrix}. \quad (2)$$

C. Approaches to modeling configurational disorder

One of the most straightforward approaches to investigate the configurational effects on the properties of alloys is to simply use a large periodic structure in which configurational disorder is simulated by randomly decorating the atomic sites to yield a target composition. Conventional methods can then be used to predict the electronic properties of these “random” structures. In principle, if the structure is large enough, it is to be expected that the ensemble of local atomic environments would approximate that of a *true* random alloy *up to a certain distance*.³⁷ Whether this distance is sufficient to accurately calculate the properties of a truly random alloy actually depends on the property to be calculated as well as the strength of the interaction between the atoms that contribute to the configurational disorder.

Instead of relying on statistical sampling methods to simulate disorder, approaches based on perturbation theory perform the configurational “averaging” analytically.³⁸ One of the most popular mean-field approaches to model configurational disorder is the coherent potential approximation (CPA)³⁹ and its variants. In the CPA, the random alloy is modeled as an ordered lattice of “effective atoms.” The coherent potential describing this effective medium is constructed by requiring that the electron scattering off the real atoms embedded in this mean field vanish on average. This robust and computationally cheap method³⁸ allows the modeling of disordered alloys with arbitrary compositions. However, given its mean-field

character, local effects, such as ion relaxations and charge transfer, are not generally taken into account.

D. Special quasirandom structures

The approaches described above suffer from important limitations. On the one hand, electronic structure calculations are quite computationally expensive and it is not practical to simulate structures with more than a few hundred atoms. On the other hand, mean-field approaches do not generally take into account effects of local ionic relaxations. Ideally, one would like to accurately calculate the thermodynamic and physical properties of random alloys—including local effects—with as small a periodic structure as possible so accurate first-principles methods can be used. This has been made possible thanks to the development of special quasirandom structures (SQS) by Zunger *et al.*¹⁸

SQS are small, *periodic* supercells that are *specially designed* to reproduce approximately the configurational structure of an infinite random alloy. The configurational state of a random alloy with a given underlying lattice and composition x can be characterized by its many-body correlation functions.¹⁸ Within the context of lattice algebra, we can assign a “spin value”— ± 1 in the case of a binary system—to each of the sites of the configuration, depending on the type of atom sitting on the site. Furthermore, all the sites can be grouped in figures, $f(k, m)$, of k vertices spanning a maximum distance of m ($m = 1, 2, 3, \dots$ is the first, second, and third-nearest neighbors, \dots). For each figure, the product of the spin variables is taken and then averaged over all the figures belonging to the same (k, m) set, yielding the correlation function, $\bar{\Pi}_{k,m}$. Rigorously, the ensemble average of a physical property can be expressed in terms of these correlation functions. The optimum SQS for a given composition is the one that best satisfies the condition

$$\langle \bar{\Pi}_{k,m} \rangle_{\text{SQS}} \cong \langle \bar{\Pi}_{k,m} \rangle_R, \quad (3)$$

where $\langle \bar{\Pi}_{k,m} \rangle_R$ is the correlation function of a random alloy, which is simply given by $(2x - 1)^k$, x being the composition in the $A_{1-x}B_x$ substitutional binary alloy. Note that in this case this constraint is only satisfied *up to a maximum range*, limited by the periodicity of the structure. It is important to note that the accuracy of the “random” properties calculated using SQS depends on the actual range of the interactions relevant to that property. This is especially true when one calculates properties that are mostly dependent on the local atomic arrangements, such as enthalpy of mixing,⁴⁰ charge transfer,³⁷ local relaxations,⁴¹ and so forth. This approach clearly fails whenever the interactions that control a given property decay slowly with distance.

Before continuing, it is highly important to stress the fact that these SQS are periodic structures. As such, they cannot, in principle, capture the physics of random alloys, particularly with respect to properties in which the lack of crystal momentum conservation, which is inherent to truly random alloys, plays a role. Despite this serious limitation, one can posit that there are some properties which are dominated by local, configurational effects. For these properties, *ab initio* calculations of the corresponding SQS may still yield useful results.

In this work, we constructed special quasirandom structures (SQS) to simulate Ti₂AlC_{1-x}N_x solid solutions, with $x = 0.25, 0.50, 0.75$.

E. Cluster expansion

When the focus is on the energetics of an alloy, we can use yet another approach to investigate the effects of configurational degrees of freedom on the thermodynamic properties of an alloy. A cluster expansion (CE) is simply a compact representation of the energetics of an alloy that can be constructed by using first-principles methods to calculate the energetics of a finite set of ordered structures with a fixed underlying lattice.⁴² Formally, a CE is defined by assigning occupation variables σ_i to each site i of a lattice (or sublattice). The occupation variables are assigned specific values (± 1 in a binary system) depending on the identity of the atom occupying the site. A particular arrangement of these “spins” corresponds to a configuration which is then represented as a vector $\vec{\sigma}$ of spins σ_i . The CE then parametrizes the energy (or any other property) of the alloy in terms of polynomial functions of the occupation variables:

$$E(\sigma) = \sum_{\alpha} m_{\alpha} J_{\alpha} \left\langle \prod_{i \in \alpha'} \sigma_i \right\rangle, \quad (4)$$

where α is a cluster (a collection of sites i). The sum is taken over all clusters α which are not equivalent by a symmetry operation of the space group of the lattice and the average is taken over all α' symmetry-equivalent clusters. The coefficients J_{α} are called the effective cluster interactions (ECIs) and relate a given configurational state to a particular energy. The multiplicities m_{α} correspond to the number of equivalent clusters (by symmetry) in a given configuration. Once the cluster expansion is found—the convergence of the expansion is highly system dependent—the energy of *any* configuration can be calculated by simply applying Eq. (4).

III. RESULTS

A. Determination of the ECIs for the cluster expansion

In this work, we have used the maps code in the ATAT package⁴² to evaluate the cluster expansion of Ti₂AlC_{1-x}N_x considering that carbon and nitrogen can exchange places in the X site. In Table I, we show the standard crystallographic parameters of the Ti₂AlC structure obtained from the ICSD database.⁴³

The cluster expansion for the Ti₂Al(C,N) system was obtained through the use of the maps code in the ATAT

TABLE I. Crystal structure parameters of Ti₂AlC.

Space Group: <i>P63/mmc</i> (194)				
Lattice Parameters: $a = b = 2.96, c = 13.22, \alpha = \beta = 90, \gamma = 120$				
Atomic Positions:				
Atom	Wyckoff Position	X	Y	Z
C,N	2a	0.0000	0.0000	0.0000
Al	2c	0.3333	0.6667	0.2500
Ti	4f	0.3333	0.6667	0.5882

TABLE II. Effective cluster interactions. The energies for the ECIs are already divided by the corresponding multiplicities.

Multiplicity	No. of Points	Cluster Diameter (Å)	Energy (meV)
1	0	0.00	-82.37
1	2	0.00	1.13
6	2	3.07	13.63
6	2	5.31	1.21
6	2	6.14	0.90
2	2	6.87	-1.42
12	2	7.52	0.78
4	3	3.07	-0.97

package.^{42,44} The unknown parameters J_{α} (effective cluster interactions, ECIs) of the cluster expansion [see Eq. (4)] can be determined by fitting them to the energy of a finite number of configurations, which in turn can be calculated using DFT approaches. The ECIs were selected based on the principle of minimization of the so-called cross-validation (CV) score, which is defined as⁴⁵

$$(CV)^2 = n^{-1} \sum_{i=1}^n (E_i - \hat{E}_{(i)}), \quad (5)$$

where E_i is the calculated energy of structure i , while $\hat{E}_{(i)}$ is the energy of the structure i obtained from the least-squares fit to the $(n - 1)$ other structures. Minimization of this CV ensures good fitting of the ECIs while ensuring that the cluster expansion retains its predictive power and avoid the pitfalls of overfitting.⁴⁵ The maps code successively increased the structure data set until the CV reached a value of less than 1 meV. Table II shows the obtained ECI parameters for the Ti₂Al(C,N) obtained in this work. A total of 69 structures were used, with energies calculated using the same methodologies described in Sec. II A. All the structures had the underlying motif of the structure described in Table I and the largest structures considered had 40 atoms per primitive cell, which is equivalent to five primitive cells.

Table II shows the calculated effective cluster interactions resulting from the cluster expansion for Ti₂Al(C,N). Excluding the empty and point ECIs, one can easily see that the first-nearest-neighbor pair ECI dominates the energetics of the system. In fact, this ECI is an order of magnitude larger than that of the remaining ECIs. Table II shows that the sole triangle ECI obtained in the present cluster expansion makes negligible contributions to the configurational energy in this system. Figure 1 shows the convergence rate of the pair ECIs as a function of cluster diameter (atom-atom distance). The figure shows that the pair ECIs converge rapidly as the cluster diameter increases. The positive values of the ECIs with smallest diameter suggest an ordering tendency between C and N in the X sublattice as it is energetically favorable to have C-N pairs.

B. (Pseudo) ground state in Ti₂Al(C,N)

Figure 2(a) compares the calculated and fitted (formation) energies (in units of kJ per formula unit) resulting from the cluster expansion and the ECIs showed in Table II. Excluding the structures with positive (formation) energies, the figure

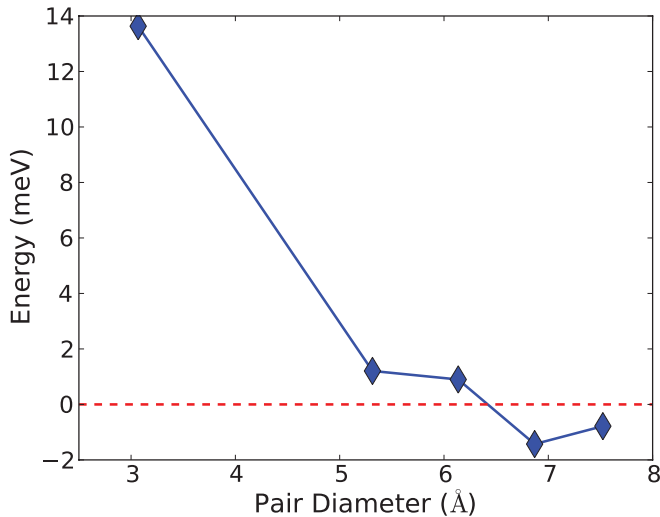


FIG. 1. (Color online) Pair effective cluster interactions (ECIs) as a function of cluster diameter.

shows very good agreement between calculated and fitted energies, as evident from the fact that all data points fall along the 45° line. Figure 2(b) shows that the uncertainty in the predicted structure energies is about ± 0.25 kJ/fu. This level of uncertainty is acceptable and it is about an order of magnitude lower than the energy scale of the system.

By sampling the configuration space generated through the search for optimal ECIs (see Table II) necessary to represent the energy of the $\text{Ti}_2\text{Al}(\text{C},\text{N})$ as a function of configuration, the “ground state”⁴⁷ of the $\text{Ti}_2\text{AlC-Ti}_2\text{AlN}$ system was determined.

Here we have used the term “pseudo” to qualify the “ground state” reported in this work because we have not considered the relative stability of $\text{Ti}_2\text{Al}(\text{C},\text{N})$ with respect to unary, binary, and other ternary compounds that may take part in equilibria in the Ti-Al-C-N system. A good example of the correct treatment of this phase stability problem is given by Dahlqvist *et al.*⁴⁶ In that work, Dahlqvist and coworkers investigated the phase stability of $\text{Ti}_2\text{AlC}_{1-x}\text{O}_x$ using SQS. To determine whether the $\text{Ti}_2\text{Al}(\text{C},\text{O})$ structures were thermodynamically stable against decomposition, they proceeded to compare their

stability with respect to other equilibrium phases in the system. The problem is essentially a linear optimization problem where the *total energy* of the system is minimized, subject to mass conservation constraints.

In this work we ignore the formal phase stability problem and assume that solutions involving $\text{Ti}_2\text{AlC-Ti}_2\text{AlN}$ or ordered structures derived from the $\text{Ti}_2\text{Al}(\text{C},\text{N})$ motif are lower in energy than competing phase equilibria involving unary, binary, ternary, and even higher order structures in the Ti-Al-C-N system. Although it is not possible to assert the validity of this assumption, the fact that solid solutions $\text{Ti}_2\text{AlC}_{1-x}\text{N}_x$ have already been synthesized experimentally⁴⁸ lends some credibility to this admittedly problematic simplification.

Although the ground-state search in this work is definitely not exhaustive, the calculations suggest ordering tendencies between C and N in the X sublattice, in agreement with the ECIs shown in Table II and Fig. 1. Figure 3 was obtained by exploring a configuration space spanning structures with up to 40 atoms per primitive cell. The resulting ground state of this system is indicated through the convex hull construction. The figure clearly shows a tendency for the $\text{Ti}_2\text{Al}(\text{C},\text{N})$ to form ordered structures *at least at low temperatures*. The lowest lying configurations have formation energies close to -5 kJ/fu. Our calculations yield six structures that fall on the convex hull. Interestingly, the ground state of the system is slightly asymmetrical, with structures rich in carbon being slightly more stable than those rich in nitrogen. The calculated convex hull does not yield any ground state at the $x = 0.5$ composition. We would like to note that Du *et al.*¹⁷ approximated a $\text{Ti}_2\text{AlC}_{0.5}\text{N}_{0.5}$ solution by simply using the primitive cell of Ti_2AlX with mixed occupancy of C and N in the X sublattice (space group: $P\bar{3}m1$). This structure, however, is well above the ground state, with a formation energy close to 1 kJ/fu. The figure also shows the formation energies calculated for $\text{Ti}_2\text{AlC}_{1-x}\text{N}_x$ SQS structures with $x = 0.25, 0.5, 0.75$. These structures are above the ground state but they have negative formation energies, indicating their stability with respect to the end members of the $\text{Ti}_2\text{Al}(\text{C},\text{N})$ system.

To gain a better understanding of the ground-state structures found in this system, the calculated electronic density of states of the ground-state structures found in Fig. 3 are shown in Fig. 4. The figure shows that all structures are

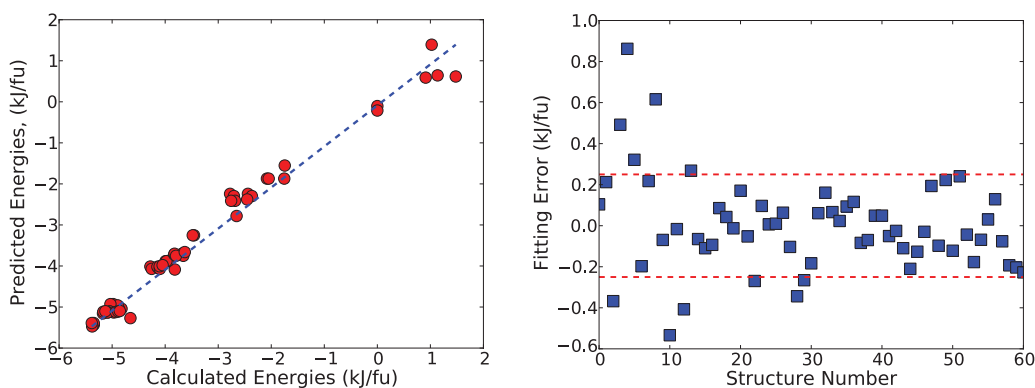


FIG. 2. (Color online) Fitting error in cluster expansion for $\text{Ti}_2\text{Al}(\text{C},\text{N})$. (a) Calculated and fitted energies resulting from the cluster expansion. These energies are calculated with respect to the Ti_2AlC and Ti_2AlN reference states. (b) Error between calculated and fitted energies resulting from the cluster expansion. ± 0.25 kJ/fu error bands are depicted with dashed lines.

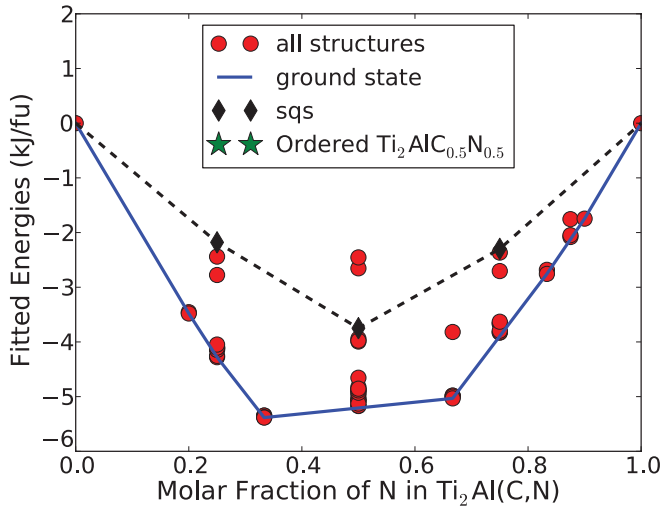


FIG. 3. (Color online) Calculation of ground state—at 0 K—for $\text{Ti}_2\text{Al}(\text{C},\text{N})$ system. [Note that in this work the full phase stability problem has been ignored and assumed that compounds along the Ti_2AlC - Ti_2AlN pseudobinary line are thermodynamically stable with respect to decomposition into combinations of other structures in the Ti-Al-C-N system. For more details see Dahlgvist (Ref. 46).] Formation energies are calculated using Ti_2AlC and Ti_2AlN as reference. The energy of the ordered structure $\text{Ti}_2\text{AlC}_{0.5}\text{N}_{0.5}$ proposed by Du *et al.* (Ref. 17) to simulate a random $\text{Ti}_2\text{AlC}_{0.5}\text{N}_{0.5}$ is shown for comparison.

metallic, with the d -band electrons from Ti ions contributing the most to the conductivity of the structures. Examining the atom-projected electronic DOS for the end member Ti_2AlC as well as the moment-projected partial electronic DOS of Ti and Al in Fig. 5 shows that the peaks centered around -1 eV correspond to hybridized p -Al and d -Ti states. These peaks become increasingly displaced to lower energies as nitrogen increasingly substitutes for carbon in the X sublattice. On the other hand, the peaks close to -2.5 eV in the electronic DOS of the Ti_2AlC correspond to hybridized p -C and d -Ti states. These very low lying states induce very strong interactions between Ti and C and result in the strong Ti-C bonds. As nitrogen substitutes for C in the X sublattice, even lower lying states—at around -5 eV—resulting from hybridization between p -N and d -Ti states begin to appear.

C. Finite-temperature alloy behavior

On a per-atom basis, the formation energy of the most stable structures (~ 1.3 kJ/atom) shown in Fig. 3 corresponds to a thermal energy of about 150 K. This suggests that despite the ordering tendencies observed, $\text{Ti}_2\text{Al}(\text{C},\text{N})$ solutions are likely to be disordered already at room temperature, which means that full long-range ordering in this system is not likely to be observed experimentally. To further explore the temperature dependence of the short-range order parameters we have used the fitted ECIs shown in Table II and Fig. 1 to investigate the finite-temperature behavior of the configuration state of this system using a simple Monte Carlo lattice simulation. Specifically, we used the ECM2 code in the ATAT package.⁴² The simulation size corresponded to an $8 \times 8 \times 8$ supercell of the

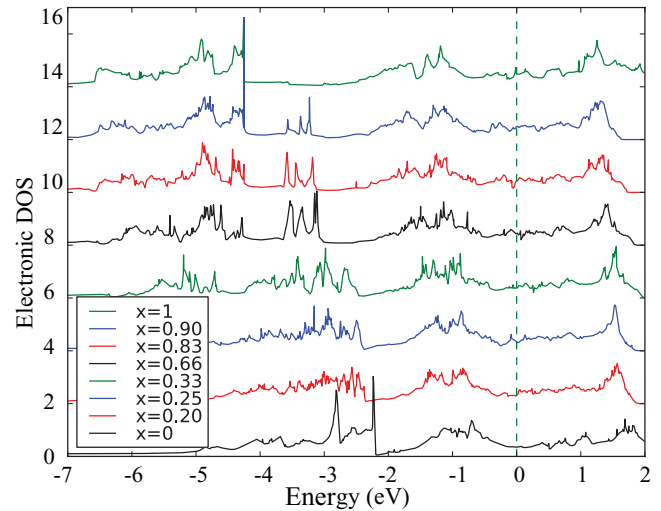


FIG. 4. (Color online) Calculated electronic density of states for the ground states in the $\text{Ti}_2\text{Al}(\text{C},\text{N})$ system depicted in Fig. 3. Bottom (top) DOS plot corresponds to the Ti_2AlC (Ti_2AlN) end members.

$\text{Ti}_2\text{Al}(\text{C},\text{N})$ primitive cell, corresponding to 1024 X sites—Ti and Al are merely expectation ions. 30 000 equilibration and 30 000 production Monte Carlo steps were used. The Monte Carlo calculations ignore electronic and vibrational contributions to the free energy of the system and it is thus likely that the temperature scale is off. When examining the ordering energies as well as the small deviations with respect to Vegard's law in the calculated volume and bulk modulus of the structures (see Figs. 8 and 9), it is not likely that vibrational effects are significant. Moreover, since all the structures are conducting, with similar electron densities at the Fermi level (see Fig. 4), electronic contributions to the free energy are also not likely to be that important. Based on these observations, we would not expect very large deviations in the calculated temperatures, although in all fairness these predictions must be taken as qualitative.

Figure 6 shows the dominant pair correlation functions—up to fourth-nearest neighbor—for the $\text{Ti}_2\text{AlC}_{0.5}\text{N}_{0.5}$ composition as a function of temperature. For this particular composition, random-like correlation functions have a value of zero. Negative pair correlation functions correspond to unlike pairs. At low temperatures, the first pair correlation function shows that carbon favors nitrogen atoms as its nearest neighbors (and vice versa). On the other hand, the second pair correlation function shows that at low temperatures next-nearest neighbors consist of like-atom pairs.

As mentioned earlier in this work, thermal energies on the order of 150–200 K are sufficient to disorder $\text{Ti}_2\text{Al}(\text{C},\text{N})$ alloys. Close inspection of Fig. 6 shows that the second, third, and fourth pair correlation functions decay to random-like values at temperatures below ~ 600 K. In fact, analyzing the local atomic configuration in snapshots of the equilibrated structure with $\text{Ti}_2\text{AlC}_{0.5}\text{N}_{0.5}$ stoichiometry simulated at 500 K, it is found that carbon has a significant preference for nitrogen as nearest-neighbor (and vice versa). On the other hand, the first pair correlation function asymptotically approaches a value below zero at much higher temperatures. These results

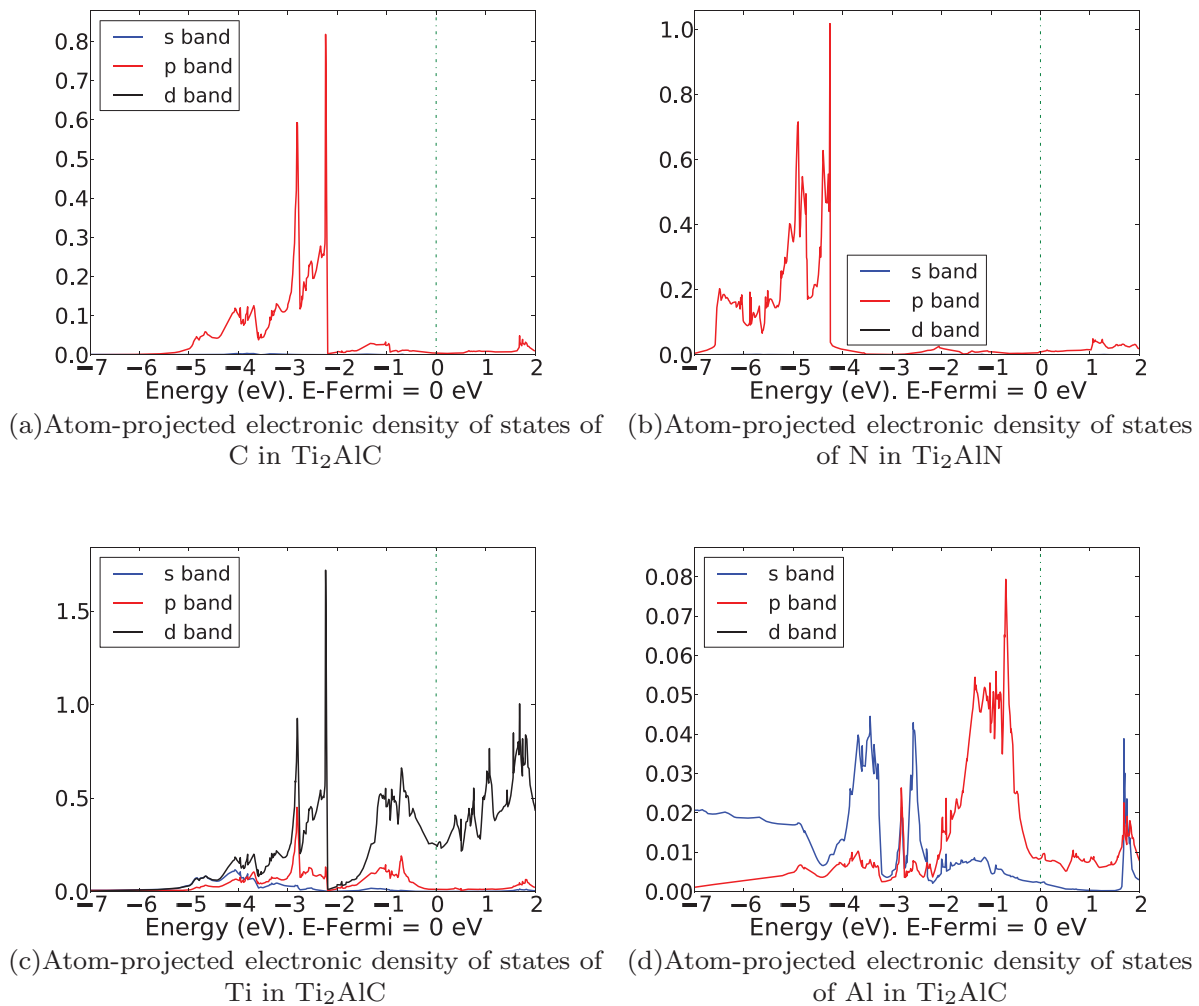


FIG. 5. (Color online) Atom-projected electronic density of states of (a) C, (c) Ti, and (d) Al in Ti_2AlC and (b) N in Ti_2AlN .

suggest that although long-range ordering is not likely to be observed in this system, short-range ordering is still somewhat significant at elevated temperatures.

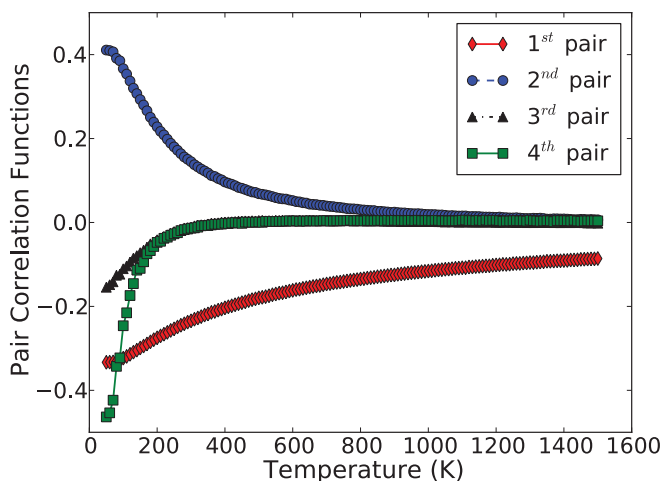


FIG. 6. (Color online) Pair correlation functions of the $Ti_2Al(C,N)$ system as a function of temperature, for the 50% N composition. Random-like correlation functions correspond to zero.

Figure 7 shows the mixing enthalpy of the $Ti_2Al(C,N)$ at 500 K calculated through Monte Carlo simulations. The temperature was chosen to ensure that no long-range ordering was significant and thus represented the mixing enthalpy of a close-to-random alloy. The figure shows that the mixing enthalpy is closely symmetrical, with some bias toward the carbon-rich region of the composition range. This is in agreement with the ground-state calculations shown in Fig. 3.

D. Structural properties of $Ti_2Al(C,N)$

The calculations in Sec. III C show that at moderate-to-elevated temperatures, $Ti_2Al(C,N)$ alloys mostly correspond to random solutions, with some degree of short-range ordering, mainly between carbon and nitrogen nearest neighbors in the X sublattice. Given that the ordering energies for this system are somewhat moderate, the ordered structures used to determine the cluster expansion are used to determine the compositional dependence of the structural properties in this system. Figure 8 shows the atomic volume for all 69 structures used to fit the ECIs in the $Ti_2Al(C,N)$ system. These volumes correspond to the fully optimized lattice parameters for each of the structures. The structures were optimized by relaxing volume, cell parameters, and internal degrees of freedom.

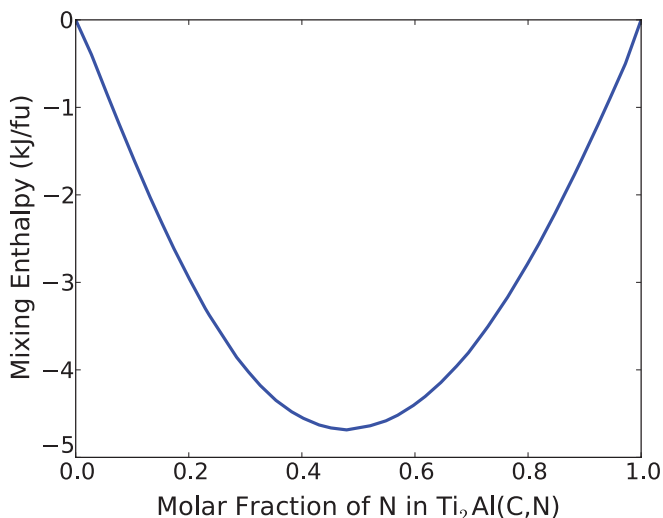


FIG. 7. (Color online) Calculated mixing enthalpy in the $Ti_2Al(C,N)$ at 500 K. Ti_2AlC and Ti_2AlN are reference states.

For convenience, the expected atomic volume in the $Ti_2Al(C,N)$ according to Vegard’s law are shown in Fig. 8. The figure shows that most of the structures have volumes that correspond to a small but *negative* deviation from Vegard’s law, with structures corresponding to the $Ti_2AlC_{0.5}N_{0.5}$ stoichiometry showing the largest deviation, in agreement with the experimental observations by Radovic *et al.*⁴⁹ According to Fig. 1, carbon and nitrogen have small but attractive interactions as nearest neighbors in the X sublattice of the carbo-nitride. This attractive interaction contributes to a shortening of C-N bonds—with respect to the weighed average of the lengths of C-C and N-N bonds in the end members. Closer inspection of the figure, however, shows that virtually all structures fall very close to the line corresponding to Vegard’s law. These small deviations from Vegard’s law are consistent with the relatively small ordering energies calculated in this system.

Figure 9 shows the calculated bulk modulus for the different ordered structures corresponding to the ground state in the

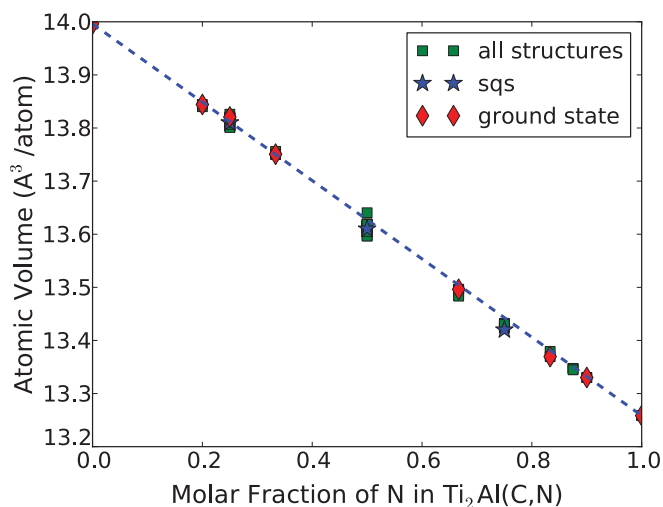


FIG. 8. (Color online) Calculated atomic volumes—in $\text{\AA}^3/\text{atom}$ —for the 69 structures used to determine the ECIs for the cluster expansion in $Ti_2Al(C,N)$.

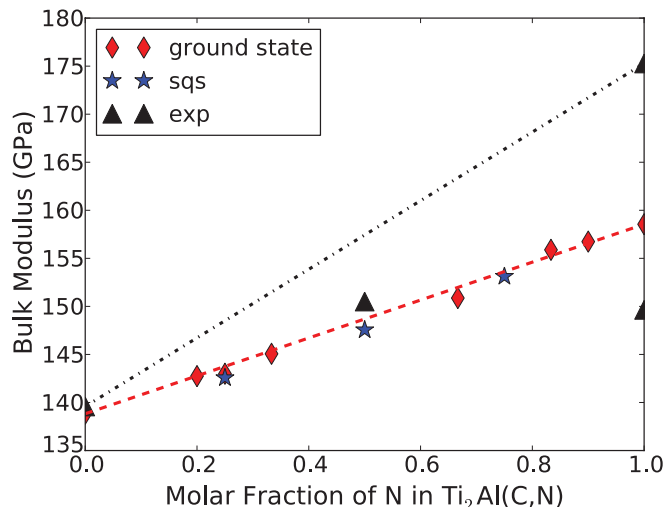


FIG. 9. (Color online) Calculated bulk modulus—in GPa—at 0 K for the structures corresponding to the ground state in $Ti_2Al(C,N)$. The experimental values are taken from the work by Radovic *et al.*⁴⁹ Note the two values for the bulk modulus for Ti_2AlN . The higher value corresponds to a sample with greater density (4.3 vs 4.245 g/cm^3), although the less dense sample is closer to the Ti_2AlN stoichiometry. See text for a more detailed discussion.

system. The bulk modulus was calculated by isotropically scaling the lattice parameters of the structures at five different volumes ranging from -5 to 5% of the equilibrium volume calculated at 0 K. The picture gets more complicated when examining the alloying behavior of the bulk modulus in the $Ti_2Al(C,N)$ system: Although the calculated bulk moduli are relatively close to the line corresponding to the (linear) rule of mixing, there is no clear trend as in the case of the volume vs composition calculations. Moreover, in the carbon-rich region of the system, the bulk modulus is a bit smaller than what could be expected from the (linear) rule of mixing; in the nitrogen-rich region there is a positive deviation. The calculated bulk modulus is in slight disagreement with the calculated volumes as one would expect that smaller volumes would result in stiffer interatomic bonds and thus larger bulk moduli.

The discrepancy between Figs. 8 and 9 may be due to the relatively small sample used to fit the equation of state for each of the structures considered. Additionally, the deviations from the expected behavior are not significant. In any case, the calculated alloying behavior for the volume and bulk modulus in the $Ti_2Al(C,N)$ system suggest that despite the tendency for this system to order, the weak C-N interactions are not sufficient to result in significant strengthening of Ti_2AlC - Ti_2AlN alloys.

The compositional behavior of the elastic constant tensor in the $Ti_2Al(C,N)$ system is shown in Fig. 10. The figure shows that the elastic constants for all the structures more or less follow the (linear) rule of mixing, with C_{11} , C_{33} , and C_{12} stiffening somewhat close to the $Ti_2AlC_{0.5}N_{0.5}$ stoichiometry. Most of the elastic constants in the system remain more or less constant as the nitrogen content increases. The most notable exception to this behavior corresponds to the C_{13} elastic constant. In this case, the stiffening of the elastic constant as the nitrogen concentration increases is notable. Whether this

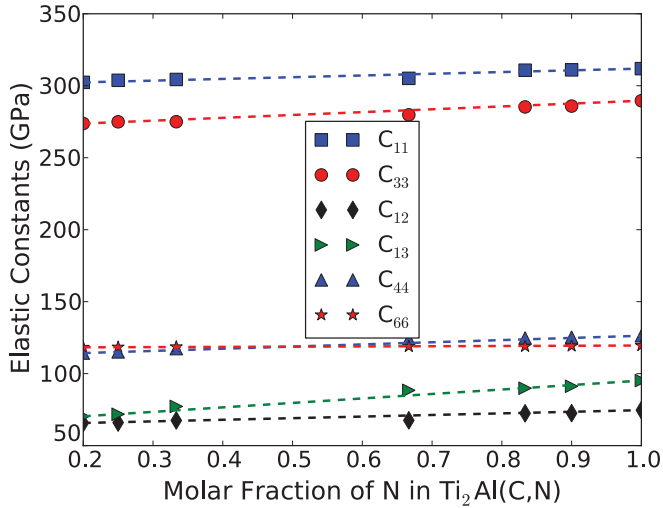


FIG. 10. (Color online) Calculated elastic constant tensor for the ground-state structures in the $\text{Ti}_2\text{Al}(\text{C},\text{N})$ system.

has consequences for the deformation behavior in this system is beyond the scope of this work but is worth investigating.

E. Special quasirandom structures in $\text{Ti}_2\text{Al}(\text{C},\text{N})$

In the previous sections, we investigated the alloying behavior of $\text{Ti}_2\text{Al}(\text{C},\text{N})$ solid solutions using the cluster expansion formalism. While this type of study has shed some light on the nature of the C-N interactions when they mix in the X sublattice as well as their effect on the thermodynamic and structural properties of these systems, it is necessary to investigate the properties of random solutions. In Sec. II D it was argued that in principle it is impossible to simulate a truly random solution with a finite set of atomic sites. A good approximation, however, can be achieved by using special quasirandom structures (SQS).

In this work we used three different special quasirandom structures representing 25, 50, and 75% N compositions. The structures were generated using the ATAT package.⁴² All structures consisted of 64 atoms. In order to simplify the structure generation, all structures were based on a $2 \times 2 \times 2$ supercell of the 8-atom primitive cell. For the structure simulating the 50% composition, the pair correlation functions were random-like up to the third-nearest-neighbor pair. In the case of the 25 (and 75) % composition structure, it was impossible to find a structure that perfectly mimicked a random solution beyond the first-nearest-neighbor pair. The structures used to calculate the properties of $\text{Ti}_2\text{AlC}_{1-x}\text{N}_x$ solid solutions with $x = 0.25, 0.50, 0.75$ are available as Supplemental Material.⁵⁰

Table III shows the calculated formation energies for SQS with three different compositions, using as reference Ti_2AlC and Ti_2AlN . Figure 3 shows that these SQS are above the ground state of the Ti_2AlC - Ti_2AlN system, although they are certainly stable with respect to decomposition into the constituent end members—i.e., they have negative formation energies. In Table III, the first formation energy (second column) corresponds to the formation energy when no local ionic relaxation is taken into account. The formation energy upon full relaxation of volume, c/a ratio, and ion positions

TABLE III. Formation energies (kJ/fu) of SQS for different relaxations. Ti_2AlC and Ti_2AlN were used as reference states.

Composition	No Local Relax.	Full Relax.	Relaxation Energy
$x_N = 0.25$	-1.95	-2.18	-0.23
$x_N = 0.50$	-2.97	-3.58	-0.60
$x_N = 0.75$	-0.96	-2.3	-1.34

is shown in the third column of the table. The table shows clearly that as the concentration of N increases, the energy gain through local ionic relaxation increases. Although in absolute terms relaxation energies are not every important, as N increases, ionic local relaxations contribute with 10, 20, and 50 %, respectively, of the formation energies for these solutions. This is important and shows that even in systems where the mixing atoms are similar in ionic radii, it is still important to consider local relaxation effects, particularly when formation energies are relatively low in magnitude.

Table IV shows the calculated lattice parameters of the end members as well as the experimental lattice parameters obtained and/or compiled by Radovic *et al.*⁴⁹ For convenience and in order to immediately detect the trends, some of these parameters are plotted in Fig. 11. The table and figure show good agreement between calculations and experiments as the the shrinkage—on a relative basis—of the a axis is larger than that of the c axis with good agreement between the theoretical

TABLE IV. Structural parameters of SQS structures. Experimental data are shown in parentheses and were taken from the work by Radovic *et al.*(Ref. 49) unless otherwise noted.

Composition	a (Å)	c (Å)	c/a	Vol. (Å ³ /atom)	B_0 (GPa)
$x_N = 0.00$	3.069	13.730	4.474	14.00	139
	(3.055)	(13.65)	(4.468)	(13.61)	(140, 186 ⁵¹)
$x_N = 0.25$	3.056	13.661	4.470	13.81	143
$x_N = 0.50$	3.037	13.631	4.488	13.61	148
	(3.023)	(13.61)	(4.50)	(13.45)	(151)
$x_N = 0.75$	3.017	13.628	4.517	13.42	153
$x_N = 1.00$	2.997	13.639	4.551	13.25	159
	(2.996)	(13.62)	(4.54)	(13.17)	(150, 175, 169 ⁵¹)

Note 1. Experimental uncertainty in lattice parameters is approximately ± 0.01 to ± 0.04 Å.

Note 2. The bulk modulus from Radovic *et al.* (Ref. 49) was obtained from their measured values of Young's (E) and shear modulus (G) and converted to bulk modulus using the formula $B = \frac{EG}{3(3G-E)}$. These measurements correspond to adiabatic conditions.

Note 3. Radovic *et al.* (Ref. 49) measurements of the elastic constants were done through resonant ultrasound spectroscopy (RUS). No temperature is reported but is assumed to be room temperature.

Note 4. The two values for the bulk modulus of Ti_2AlN correspond to two different samples (see text).

Note 5. The bulk modulus reported in Manoun *et al.* (Ref. 51) were obtained using a diamond anvil cell (DAC). No temperature is reported but is assumed to be room temperature. Uncertainty in experiments is about ± 3 GPa. These experiments were performed under close-to-isothermal conditions.

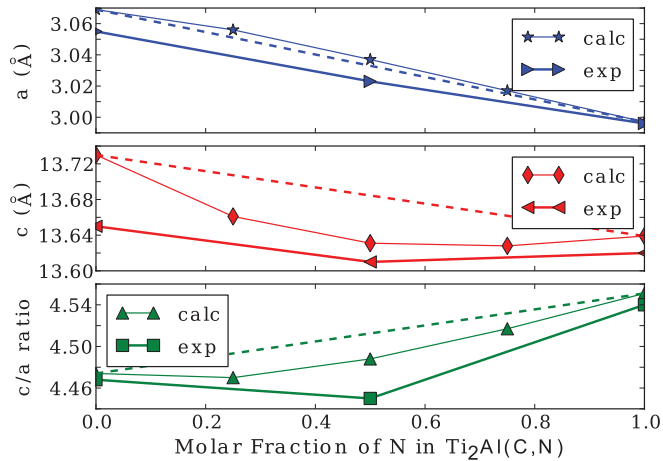


FIG. 11. (Color online) Lattice parameters of the SQS structures compared with end members Ti_2AlC and Ti_2AlN .

and experimental observations.⁴⁹ Table IV and Fig. 11 also show that as nitrogen substitutes carbon, the a axis shrinks, although the compositional trend follows closely Vegard's law. On the other hand, replacing carbon with nitrogen leads to a reduction in the c axis after which this parameter increases again toward the N-rich region of the composition range. The same can be observed in the plot of the c/a ratio shown in the same Fig. 11. The stronger deviation from Vegard's law in the case of the c axis may be due to the stronger M-X interactions that result from carbon and nitrogen mixing in the X sublattice. As shown in Sec. III B, there is also a net attractive interaction between C and N as they start to mix in the X sublattice.

Table IV also shows the calculated—at 0 K—and experimental^{49,51}—assumed at room temperature—bulk modulus (B_0) for $\text{Ti}_2\text{Al}(\text{C},\text{N})$ solid solutions. The experimental data from Manoun *et al.*⁵¹ were obtained from diamond anvil experiments while those reported by Radovic *et al.*⁴⁹ used resonant ultrasound spectroscopy (RUS) techniques. Immediately, we can see a rather large and qualitatively important difference between both experimental data sets: Discrepancies in the measured bulk modulus for Ti_2AlC reach close to 50 GPa. One could argue that the bulk moduli reported in both sets of experiments are fundamentally different thermodynamic quantities as one corresponds to isothermal (diamond anvil) while the other one corresponds to adiabatic (RUS) conditions. However, at room temperature it is unlikely that adiabatic and isothermal bulk moduli differ by such a large range. More importantly, the diamond anvil experiments suggest that the bulk modulus of Ti_2AlC is actually larger than that of Ti_2AlN . This result is clearly in conflict with the more recent RUS results from Radovic *et al.*⁴⁹ as well as with the calculations. In recent work by the author and collaborators,⁵² it is argued that the larger bulk modulus of Ti_2AlN is due to the stronger covalent character of Ti-N bonds in Ti_2AlN . This is also consistent with the shorter Ti-X bonds in Ti_2AlN . Here we would like to note that the values for the bulk modulus of Ti_2AlN reported by Radovic *et al.*⁴⁹ in Table IV correspond to two samples. The sample with higher density (4.3 g/cm³) had a stoichiometry corresponding to $\text{Ti}_{1.93}\text{AlN}_{0.975}$, while the

sample with lower density (4.245 g/cm³) had a stoichiometry corresponding to $\text{Ti}_2\text{AlN}_{0.996}$, which is closer to Ti_2AlN . The densities and stoichiometries of the samples are in conflict, which could be explained by different degrees of porosity. In this work, we assume that the bulk modulus of the denser sample is closer to the true bulk modulus of materials close to the Ti_2AlN stoichiometry, although further investigation is warranted.

In Sec. III D, it was noted that the observed alloying behavior of the bulk modulus does seem to be in contradiction with the observed (slight) negative deviations from the (linear) rule of mixing in the compositional dependence of the volume (see Fig. 9). In Fig. 9 it is shown that the ordered structures belonging to the ground state have bulk moduli that follow closely the (linear) rule of mixing, although the deviations are *negative* in the carbon-rich region of the composition range. The calculations for the SQS structures also show essentially the same thing: Despite the fact that C-N alloying results in shorter bonds (smaller volume) relative to the weighed average of the end members, the bulk modulus actually *decreases*—relative to the (linear) rule of mixing—as nitrogen substitutes carbon. Table IV and Fig. 9 show that the experimental results are somewhat inconclusive. In their work, Radovic *et al.*⁴⁹ prepared two different samples of nominal Ti_2AlN that actually had very different concentration levels of point defects (nitrogen vacancies). The sample with the highest density (4.3 vs 4.245 g/cm³) showed a much higher bulk modulus that agreed somewhat better with the theoretical results. On the other hand, the sample with the lowest density showed a remarkable softening of about 25 GPa. We would like to note that the higher values of the bulk modulus obtained by Radovic *et al.*⁴⁹ for one of the Ti_2AlN samples agree better with the anvil experiments by Manoun *et al.*⁵¹

If we only consider the highest density sample for Ti_2AlN and compare the experimental and calculated trends in Fig. 9, we can clearly see that there is good agreement between experiments and calculations: Despite the fact that on average there are shorter bonds at intermediate compositions—again, relative to the (linear) rule of mixing—we can see a softening of the bulk modulus relative to the weighed average of the bulk modulus for Ti_2AlC and Ti_2AlN . The reason for this negative deviation from the (linear) rule of mixing is not entirely clear at this moment but it is likely related to changes in the bonding behavior between Ti-Al, T-X, and X-X atoms as carbon and nitrogen mix in the X sublattice. This explanation is admittedly unsatisfactory and one must also consider the softening observed in one of the two samples of Ti_2AlN examined by Radovic *et al.*⁴⁹ It is very likely that this softening is induced by point defects but since in this work the formation of nitrogen vacancies was not considered it is not possible to make a stronger assertion regarding the underlying effect of alloying on the properties of $\text{Ti}_2\text{Al}(\text{C},\text{N})$ solid solutions *close to the nitrogen-rich region of the composition range*.

IV. SUMMARY AND CONCLUSIONS

In this work, we have investigated the alloying behavior of $\text{Ti}_2\text{Al}(\text{C},\text{N})$ solid solutions through theoretical means. The following are some of the most important results obtained in this work:

(1) A cluster expansion describing the chemical interactions between C and N in the X sublattice was built by fitting the effective cluster interactions (ECIs) of the expansion to the calculated energies of 69 structures derived from Ti_2AlC .

(2) A ground-state search using this cluster expansion showed ordering tendency between C and N, and several ground states—with up to 40 atoms per primitive unit cell—were identified.

(3) The ordering tendency is not significant and it is likely that the system loses long-range order at 500–600 K. Calculations of the temperature evolution of pair correlation functions for the $\text{Ti}_2\text{AlC}_{0.5}\text{N}_{0.5}$ stoichiometry seem to corroborate this.

(4) Using the calculated structural properties of the structures used to determine the cluster expansion, we found a shortening of the average interatomic distances upon C-N alloying, relative to Vegard's law.

(5) The elastic properties of the structures considered seem to follow closely the (linear) rule of mixing, with some deviation as the alloying progresses. Paradoxically, while alloying seems to result in shorter interatomic distances, the bulk modulus of structures corresponding to C-N alloying shows negative deviations from the (linear) rule of mixing, which implies a net softening of the solid solution upon alloying.

(6) Solid solutions were simulated through the use of special quasirandom structures (SQS) and the results are basically in agreement with those obtained using ordered structures with an underlying $\text{Ti}_2\text{Al}(\text{C},\text{N})$ motif.

(7) Some experimental results seem to suggest that this alloying-mediated softening is real, although no conclusive statement can be made due to the fact that point defects may play a very significant role in determining the properties of these solid solutions.

ACKNOWLEDGMENTS

R. Arróyave acknowledges the support from NSF through Grant Nos. CMMI-0758298, 1027689, 0953984, 0900187, and DMR-0805293. First-principles calculations were carried out in the Chemical Engineering Cluster and the Texas A&M Supercomputing Facility at Texas A&M University as well as in the Ranger Cluster at the Texas Advanced Computing Center at University of Texas, Austin. Preparation of the input files and analysis of the data have been performed within the framework AFLOW/ACONVASP⁵³ developed by Stefano Curtarolo as well as with the ATAT package⁴⁴ developed by Axel van de Walle.

*rroyave@tamu.edu

¹M. W. Barsoum, *Prog. Solid State Chem.* **28**, 201 (2000).

²M. W. Barsoum and M. Radovic, in *Encyclopedia of Materials: Science and Technology*, edited by K. H. J. Buschow, R. Cahn, M. Flemings, B. Ilshner, E. Kramer, S. Mahajan, and P. Veysiere (Elsevier, Oxford, 2004), pp. 1–16.

³M. Barsoum and M. Radovic, *Annu. Rev. Mater. Res.* **41**, (2011).

⁴Z. M. Sun, *Int. Mater. Rev.* **56**, 143 (2011).

⁵M. W. Barsoum, D. Brodtkin, and T. El-Raghy, *Scripta Mater.* **36**, 535 (1997).

⁶A. Zhou, M. Barsoum, S. Basu, S. Kalidindi, and T. El-Raghy, *Acta Mater.* **54**, 1631 (2006).

⁷M. Radovic, M. W. Barsoum, A. Ganguly, T. Zhen, P. Finkel, S. R. Kalidindi, and E. Lara-Curzio, *Acta Mater.* **54**, 2757 (2006).

⁸B. Manoun, F. X. Zhang, S. K. Saxena, T. El-Raghy, and M. W. Barsoum, *J. Phys. Chem. Solids* **67**, 2091 (2006).

⁹V. D. Jovic, M. W. Barsoum, B. M. Jovic, A. Ganguly, and T. El-Raghy, *J. Electrochem. Soc.* **153**, B238 (2006).

¹⁰A. Ganguly, M. Barsoum, and R. Doherty, *J. Amer. Ceram. Soc.* **90**, 2200 (2007).

¹¹N. Haddad, E. Garcia-Caurel, L. Hultman, M. W. Barsoum, and G. Hug, *J. Appl. Phys.* **104**, 023531 (2008).

¹²S. Amini, C. Ni, and M. W. Barsoum, *Composites Sci. Tech.* **69**, 414 (2009).

¹³A. G. Zhou and M. W. Barsoum, *J. Alloys Compd.* **498**, 62 (2010).

¹⁴N. J. Lane, S. C. Vogel, and M. W. Barsoum, *J. Amer. Ceram. Soc.* **94**, 3473 (2011).

¹⁵M. K. Drulis, H. Drulis, A. E. Hackemer, A. Ganguly, T. El-Raghy, and M. W. Barsoum, *J. Alloys Compd.* **433**, 59 (2007).

¹⁶T. Scabarozzi, A. Ganguly, J. D. Hettinger, S. E. Lofland, S. Amini, P. Finkel, T. El-Raghy, and M. W. Barsoum, *J. Appl. Phys.* **104**, 073713 (2008).

¹⁷Y. L. Du, Z. M. Sun, H. Hashimoto, and M. W. Barsoum, *Phys. Lett. A* **374**, 78 (2009).

¹⁸A. Zunger, S. H. Wei, L. G. Ferreira, and J. E. Bernard, *Phys. Rev. Lett.* **65**, 353 (1990).

¹⁹W. Kohn and L. J. Sham, *Phys. Rev.* **140**, A1133 (1965).

²⁰G. Kresse and J. Furthmüller, *Phys. Rev. B* **54**, 11169 (1996).

²¹G. Kresse and J. Furthmüller, *Comput. Mater. Sci.* **6**, 15 (1996).

²²J. P. Perdew, K. Burke, and M. Ernzerhof, *Phys. Rev. Lett.* **77**, 3865 (1996).

²³J. P. Perdew, K. Burke, and M. Ernzerhof, *Phys. Rev. Lett.* **78**, 1396 (1997).

²⁴P. E. Blöchl, *Phys. Rev. B* **50**, 17953 (1994).

²⁵J. Hafner, *Comput. Phys. Commun.* **177**, 6 (2007).

²⁶J. Hafner, *J. Comput. Chem.* **29**, 2044 (2008).

²⁷H. J. Monkhorst and J. D. Pack, *Phys. Rev. B* **13**, 5188 (1976).

²⁸M. Methfessel and A. T. Paxton, *Phys. Rev. B* **40**, 3616 (1989).

²⁹P. E. Blöchl, O. Jepsen, and O. K. Andersen, *Phys. Rev. B* **49**, 16223 (1994).

³⁰S. Ganeshan, S. L. Shang, Y. Wang, and Z. K. Liu, *Acta Mater.* **57**, 3876 (2009).

³¹S. Ganeshan, S. L. Shang, H. Zhang, Y. Wang, M. Mantina, and Z. K. Liu, *Intermetallics* **17**, 313 (2009).

³²D. E. Kim, S. L. Shang, and Z. K. Liu, *Comput. Mater. Sci.* **47**, 254 (2009).

³³Y. Le Page and P. Saxe, *Phys. Rev. B* **65**, 104104 (2002).

³⁴S. L. Shang, G. Sheng, Y. Wang, L. Q. Chen, and Z. K. Liu, *Phys. Rev. B* **80**, 052102 (2009).

- ³⁵S. Shang, Y. Wang, and Z. K. Liu, *Appl. Phys. Lett.* **90**, 101909 (2007).
- ³⁶J. X. Zhang, Y. L. Li, Y. Wang, Z. K. Liu, L. Q. Chen, Y. H. Chu, F. Zavaliche, and R. Ramesh, *J. Appl. Phys.* **101**, 114105 (2007).
- ³⁷S. H. Wei, L. G. Ferreira, J. E. Bernard, and A. Zunger, *Phys. Rev. B* **42**, 9622 (1990).
- ³⁸P. E. A. Turchi, I. A. Abrikosov, B. Burton, S. G. Fries, G. Grimvall, L. Kaufman, P. Korzhavyi, V. Rao Manga, M. Ohno, and A. Pisch, *CALPHAD* **31**, 4 (2007).
- ³⁹F. Yonezawa, K. Morigaki, and T. Matsubara, editors, *Structure and Properties of Matter* (Springer, Berlin, 1982), p. 383.
- ⁴⁰D. Shin, R. Arróyave, Z. K. Liu, and A. Van de Walle, *Phys. Rev. B* **74**, 024204 (2006).
- ⁴¹A. V. Ruban, S. I. Simak, S. Shallcross, and H. L. Skriver, *Phys. Rev. B* **67**, 214302 (2003).
- ⁴²A. Van de Walle, M. Asta, and G. Ceder, *CALPHAD* **26**, 539 (2002).
- ⁴³A. Belsky, M. Hellenbrandt, V. L. Karen, and P. Luksch, *Acta Crystallogr. Sect. A* **58**, 364 (2002).
- ⁴⁴A. van de Walle, *CALPHAD* **33**, 266 (2009).
- ⁴⁵A. van de Walle and G. Ceder, e-print [arXiv:cond-mat/0201511](https://arxiv.org/abs/cond-mat/0201511).
- ⁴⁶M. Dahlqvist, B. Alling, I. A. Abrikosov, and J. Rosén, *Phys. Rev. B* **81**, 024111 (2010).
- ⁴⁷Strictly speaking, the search for the true ground state of a chemical system is a problem without solution due to the impossibility of completely sampling the entire configurational space. Even if this problem could be overcome, only by establishing the relative stability of these structures in competition with all the possible unary, binary, and other ternary and higher order structures in the $\text{Ti}_2\text{Al}(\text{C},\text{N})$ system can one really determine the (pseudo) ground state of the system.
- ⁴⁸B. Manoun, S. K. Saxena, G. Hug, A. Ganguly, E. N. Hoffman, and M. W. Barsoum, *J. Appl. Phys.* **101**, 113523 (2007).
- ⁴⁹M. Radovic, A. Ganguly, and M. W. Barsoum, *J. Mater. Res.* **23**, 1517 (2008).
- ⁵⁰See Supplemental Material at <http://aps.org/supplemental/10.1103/PhysRevB.84.134112> for .txt files containing the lattice vectors and atomic coordinates of the SQS structures used to simulate random solutions of $\text{Ti}_2\text{Al}(\text{C},\text{N})$ 25, 50, and 75% N. The structures are formatted as INCAR files to be used with the VASP code.
- ⁵¹B. Manoun, F. X. Zhang, S. K. Saxena, T. El-Raghy, and M. W. Barsoum, *J. Phys. Chem. Solids* **67**, 2091 (2006).
- ⁵²T. Duong, S. Gibbons, R. Kinra, and R. Arróyave, *J. Appl. Phys.* (in press, 2011).
- ⁵³W. Setyawan and S. Curtarolo, *Comput. Mater. Sci.* **49**, 299 (2010).